



Supplement of

A qualitative comparison of secondary organic aerosol yields and composition from ozonolysis of monoterpenes at varying concentrations of NO₂

D. C. Draper et al.

Correspondence to: J. L. Fry (fry@reed.edu)

The copyright of individual parts of the supplement might differ from the CC-BY 3.0 licence.

Supplemental Information

Kinetics Modeling

To account for uncertainties in measured NO_2 concentrations and to constrain BVOC concentrations during experiments, each experiment was modeled to estimate the full time series of each species as well as to simulate the 1st generation oxidation chemistry.

A simple kinetics box model was written to iteratively solve the differential rate laws for each species expected to be present in the chamber and to mimic the steady state flow conditions (constant addition and dilution) of the chamber, assuming instantaneous mixing. We start each model run allowing either O_3 or $\text{O}_3 + \text{NO}_2$ to reach steady state in the chamber. The laboratory O_3 source is highly stable and thus matched well by the same initial parameters (flask concentration, flow rate) for every experiment. During this oxidant stabilization period, NO_2 is the only chemical sink for O_3 , so we are able to tune the NO_2 source concentration until the modeled and observed O_3 time series match. This period is shown in Figure S.1 in the shaded region. Once oxidant stabilization is achieved, BVOC is added. BVOC addition causes O_3 to decay faster, now from both direct reaction with BVOC and additional NO_3 formation from $\text{O}_3 + \text{NO}_2$. Since $[\text{NO}_2]$ is well characterized by the time BVOC is added, the BVOC source concentration is the only parameter that needs to be adjusted to match this final O_3 decay (unshaded region in Figure S.1).

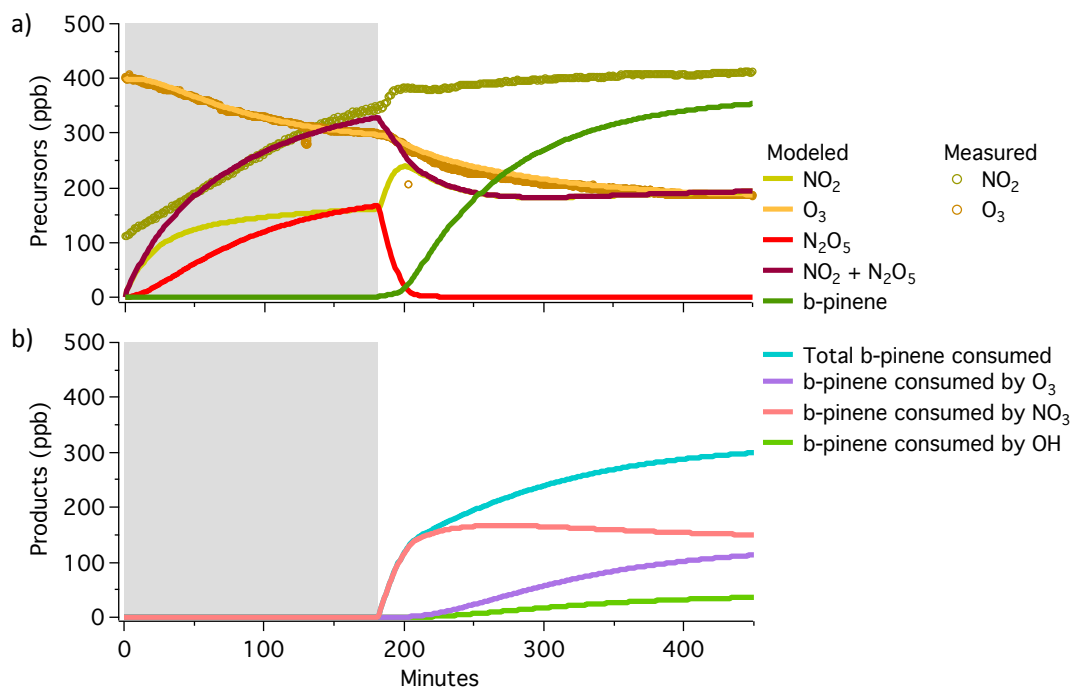


Figure S.1. Sample model run of β -pinene with the lowest NO_2 concentration showing agreement between modeled and measured O_3 and modeled $\text{NO}_2 + \text{N}_2\text{O}_5$ to measured NO_2 (a, shaded region); agreement between measured and modeled O_3 following the

addition of β -pinene (a, unshaded region), and the instantaneous concentrations of bulk oxidation products from each oxidant (b).

The full list of rate constants used is described in Table S.1. Explicit kinetics data exists for all of the initial stages of chemistry (inter-oxidant reactions and BVOC oxidation). While these rate constants, for e.g. BVOC + NO₃, are based on a small number of measurements and thus have uncertainty of order 20 % associated with them, the least certain rate constants used here are those describing the fate of the RO₂ radical formed following BVOC oxidation, which vary by orders of magnitude.

Table S.1. Rate constants used in kinetics model.

Reaction	k (298 K) (cm ³ molec ⁻¹ s ⁻¹ unless otherwise indicated)	Ref.
NO ₂ + O ₃ + M → NO ₃ + O ₂ + M	3.5 × 10 ⁻¹⁷	Atkinson et al. (2004)
NO ₂ + NO ₃ → N ₂ O ₅	1.18 × 10 ⁻¹²	Sander et al. (2011)
N ₂ O ₅ → NO ₂ + NO ₃	0.041 s ⁻¹	Sander et al. (2011)
OH + NO ₂ + M → HNO ₃ + M	1.1 × 10 ⁻¹¹	DeMore et al. (1994)
OH + HNO ₃ → NO ₃ + H ₂ O	2.7 × 10 ⁻³⁹	DeMore et al. (1994)
NO + NO ₃ → 2 NO ₂	2.6 × 10 ⁻¹¹	DeMore et al. (1994)
NO + O ₃ → NO ₂ + O ₂	1.8 × 10 ⁻¹⁴	DeMore et al. (1994)
NO ₃ + BVOC → products (assumed RO ₂) BVOC = α -pinene β -pinene Δ -carene limonene	6.2 × 10 ⁻¹² 2.51 × 10 ⁻¹² 9.1 × 10 ⁻¹² 1.22 × 10 ⁻¹¹	Atkinson and Arey (2003)
O ₃ + BVOC → products (assumed RO ₂) BVOC = α -pinene β -pinene Δ -carene limonene	8.4 × 10 ⁻¹⁷ 1.5 × 10 ⁻¹⁷ 3.7 × 10 ⁻¹⁷ 2.1 × 10 ⁻¹⁶	Atkinson and Arey (2003)
OH + BVOC → products (assumed RO ₂) BVOC = α -pinene β -pinene Δ -carene limonene	5.23 × 10 ⁻¹¹ 7.43 × 10 ⁻¹¹ 8.8 × 10 ⁻¹¹ 1.64 × 10 ⁻¹⁰	Atkinson and Arey (2003)

$\text{O}_3 + \text{BVOC} \rightarrow \text{OH}$ BVOC = α -pinene β -pinene Δ -carene limonene	$0.85 \times (8.4 \times 10^{-17})$ $0.35 \times (1.5 \times 10^{-17})$ $1.06 \times (3.7 \times 10^{-17})$ $0.86 \times (2.1 \times 10^{-16})$	Atkinson and Arey (2003) (O_3 rate constants); Atkinson et al. (1992) (OH yields)
$\text{RO}_2 + \text{RO}_2 \rightarrow \text{products}$	$1 \times 10^{-15} - 1 \times 10^{-12}$	Ziemann and Atkinson (2012); Ehn et al. (2014); Orlando and Tyndall (2012); Lightfoot et al. (1992)
$\text{RO}_2 + \text{NO}_3 \rightarrow \text{products}$	2×10^{-12}	Vaughan et al. (2006); Orlando and Tyndall (2012)
$\text{RO}_2 + \text{NO}_2 \rightarrow \text{ROONO}_2$	4.8×10^{-11}	Sander et al. (2011)
$\text{ROONO}_2 \rightarrow \text{RO}_2 + \text{NO}_2$	22 s^{-1}	Sander et al. (2011)

The three most likely reaction partners to RO_2 radicals in these experiments are RO_2 , NO_3 , and NO_2 . HO_2 chemistry is not incorporated into the model, as we expect mainly tertiary RO_2 to form and thus negligible HO_2 production (Atkinson, 1997). We note that this lack of HO_2 is a significant deviation from the real atmosphere where nighttime HO_2 concentrations can be comparable to RO_2 concentrations (Wolfe et al., 2014; Andres-Hernandez et al., 2013). In these experiments, we understand the relative rate constants of $\text{RO}_2 + \text{RO}_2$ and $\text{RO}_2 + \text{NO}_3$ to be the most substantial driver of how much BVOC reacts in the NO_2 -influenced experiments because they determine how much NO_3 remains available to react with BVOC. $\text{RO}_2 + \text{NO}_2$ will affect both the RO_2 reservoir as well as NO_3 formation potential, but since the products (ROONO_2) are understood to be fairly unstable (Sander et al., 2011), they decompose quickly back into RO_2 and NO_2 and thus are not as directly influential on [BVOC]. The $\text{RO}_2 + \text{NO}_3$ rate constant has been measured to be $(1.8 \pm 1.5) \times 10^{-12} \text{ cm}^3 \text{ molec}^{-1} \text{ s}^{-1}$ for multiple RO_2 ranging from C_2 to C_6 , so we approximate to $2 \times 10^{-12} \text{ cm}^3 \text{ molec}^{-1} \text{ s}^{-1}$ in this study. It has not been measured for the RO_2 radicals expected to be in this system, but the rate constant does not seem to show a strong dependence on size or branching of the RO_2 and thus the molecules for which it has been measured are likely a good proxy for the chemistry here (Vaughan et al., 2006). The $\text{RO}_2 + \text{RO}_2$ rate constants that have been measured, however, are much more variable. Examination of trends in the literature shows that increasing the size (# C atoms) of the RO_2 radical can increase its self-reaction rate constant by multiple orders of magnitude; increasing branching of the RO_2 (from primary to tertiary) decreases the rate constant by multiple orders of magnitude; functional group substitution at the β -carbon can increase the rate constant by up to two orders of

magnitude (Ziemann and Atkinson, 2012; Orlando and Tyndall, 2012; Lightfoot et al., 1992).

In each monoterpene system, we expect to be making mainly tertiary, NO_3 -functionalized C_{10} RO_2 . Having a β -nitrato tertiary RO_2 gives us our low estimate of the $\text{RO}_2 + \text{RO}_2$ rate constant ($k = 1 \times 10^{-15} \text{ cm}^3 \text{ molec}^{-1} \text{ s}^{-1}$) (Ziemann and Atkinson, 2012; Atkinson, 1997). These C_{10} peroxy radicals are at least 4 carbons bigger than any with measured rate constants, though, and thus it is entirely possible that the real rate constant is a few orders of magnitude higher. For this study we choose $k = 1 \times 10^{-12} \text{ cm}^3 \text{ molec}^{-1} \text{ s}^{-1}$ as a reasonable upper limit, since it has been supported by measurements of product formation (Ehn et al., 2014). This difference of 3 orders of magnitude dominates the uncertainty for this modeling approach. Using each of these two bounding $\text{RO}_2 + \text{RO}_2$ rate constants, we can then determine the BVOC source concentration that matches the observed O_3 decay, thus giving us a best estimate range of [BVOC].

Once the precursor concentrations are decided upon, the percentage of BVOC reacted by each oxidant is calculated within the model (Figure S.2). Since no OH scavenger was used during experiments, we assume that stabilized Criegee intermediates from ozonolysis produced OH at the yields reported by (Atkinson et al., 1992; shown in Table S.1).

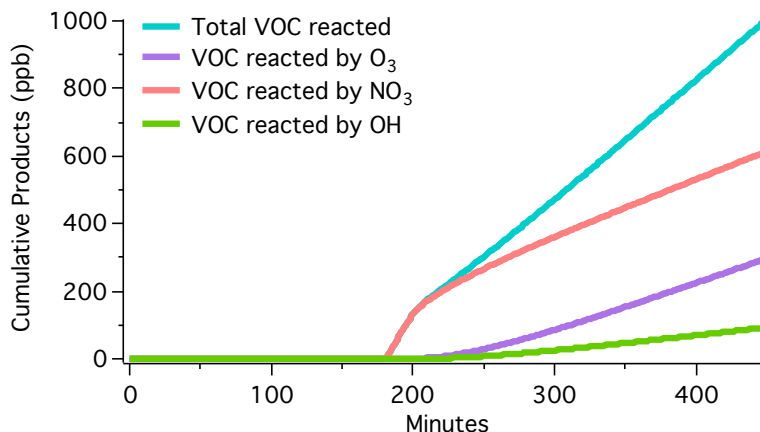


Figure S.2. Sample model run of β -pinene with the lowest NO_2 concentration showing the cumulative oxidation products from each oxidant.

BVOC measurement and characterization of uncertainties

As described in the main body of the text, the BVOC delivery system was designed to maintain a constant vapor pressure of the BVOC in the source flask, which could then be flowed continuously into the chamber. This constant vapor pressure was achieved by injecting a small ($<0.2 \text{ mL}$) liquid sample of the monoterpene into a flask submerged into a chiller bath held at the appropriate temperature to give a concentration of 100 ppm in the headspace of the flask (Figure S.3). This methodology relies on several assumptions. We assume that the vapor pressure-driven concentration (and temperature) inside the flask reaches equilibrium within the residence time of gas in the flask. (14 mL/min air flow through a 100 mL flask $\approx 7 \text{ min}$). We also assume that the surface area of the liquid sample remains constant over time.

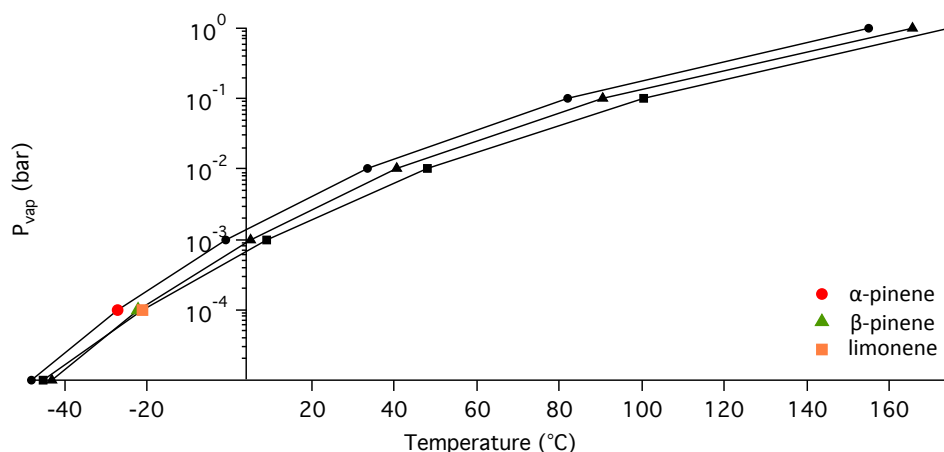


Figure S.3. Temperature dependence of vapor pressure of α -pinene, β -pinene, and limonene (Haynes et al., 2012). Δ -3-carene is assumed to reach the target vapor pressure at -25 °C, between α -pinene and β -pinene.

To obtain an independent estimate of what the actual gas-phase chamber concentrations were during each experiment, data was fit using the gas-phase kinetics model described above, where NO_2 and BVOC are both tunable to fit the observed O_3 decay. The largest source of uncertainty in the model affecting the predicted BVOC concentration is the $\text{RO}_2 + \text{RO}_2$ rate constant. We chose a range shown in Table S.1, spanning three orders of magnitude in $k_{\text{RO}_2 + \text{RO}_2}$, which predicts a range of BVOC concentrations that varies by no more than about 25%. This source of uncertainty drives our precision estimate for the amount of BVOC consumed and is incorporated into yield calculations in Section 3.2 and shown in Figure 4. Here the BVOC time series generated by using each of the low and high $k_{\text{RO}_2 + \text{RO}_2}$ values were averaged together for each individual experiment, and the standard deviation was taken to be the error on the ΔHC values.

Additionally, the model calculates the BVOC concentration assuming a single BVOC + oxidant reaction, and therefore limonene's ΔHC may be an overestimate since limonene has two double bonds that can potentially react with O_3 or NO_3 (Zhang et al., 2006).

Wall loss characterization

Aerosol wall losses in this chamber were characterized according to the method employed by previous studies (McMurry et al., 1985; Fry et al., 2014). An approximately 0.02 M solution of $(\text{NH}_4)_2\text{SO}_4$ was atomized, dried through a diffusion dryer, and measured directly into the SEMS to obtain a known input aerosol distribution. The concentration of the seed solution was optimized to span the full size range (20-800 nm) of aerosol that was observed during experiments. The seed aerosol at the same flow rate was then introduced into the chamber and measured with the SEMS at the outlet of the chamber (Figure S.5a). First order size-dependent wall loss coefficients, $\beta(D_p)$, were

calculated according to Eq. 1, using average size distributions going into (N_{in}) and coming out of the chamber (N_{out}), the chamber flow rate (Q), chamber volume (V), and assuming the chamber to behave as a continuously stirred tank reactor.

$$\beta(D_p) = \left(\frac{Q}{V}\right) \left[\left(\frac{N_{in}(D_p)}{N_{out}(D_p)} \right) - 1 \right] \quad (1)$$

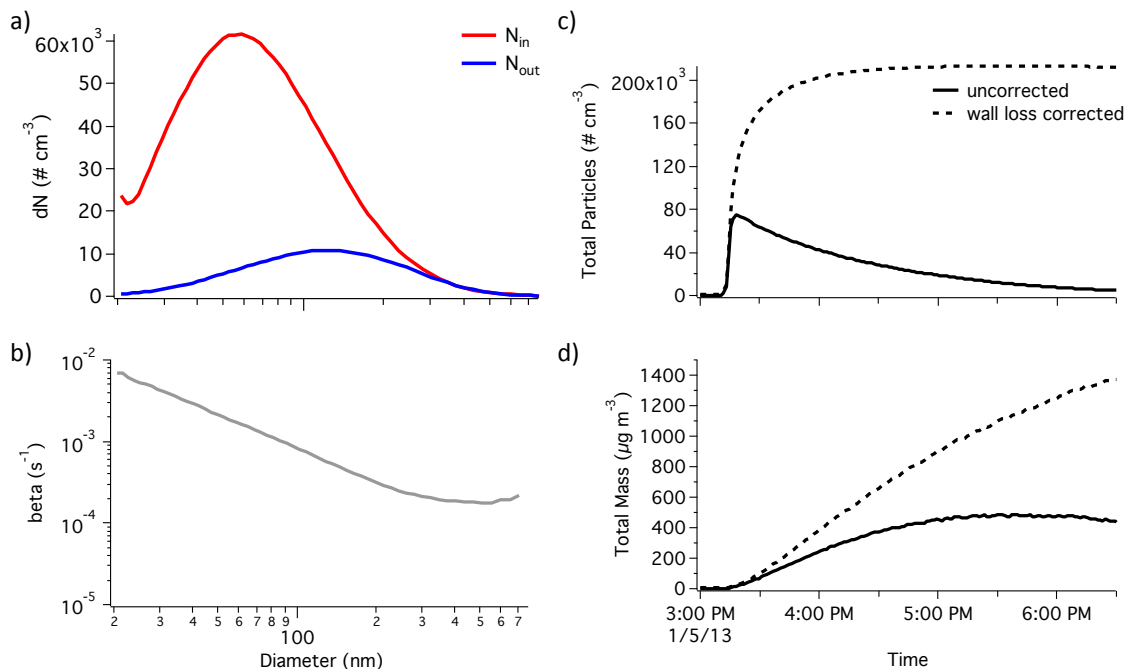


Figure S.5. (a) Input and output number size distributions of the seed aerosol entering and leaving the chamber; (b) Size-dependent wall loss rates; Uncorrected and corrected time series of total aerosol number concentrations (c) and mass (d) from a representative experiment (α -pinene + O_3).

Raw size distributions from experiments were corrected cumulatively for wall losses (McMurry et al., 1985; Fry et al., 2014). At each time step, loss rates were multiplied by the raw size distribution to determine how many particles in each size bin were lost to the walls. These losses were then added back to the corrected dataset. This process assumes that any particle lost to the walls remains there and does not grow past the size it was when it was lost. This method provides reasonable corrections for total mass and total number of particles produced, but adding back static sized particles obscures observed growth dynamics. Figure S.6 shows a representative uncorrected and corrected growth event, illustrating how the particles added back remain at the size they were when they were lost to the walls.

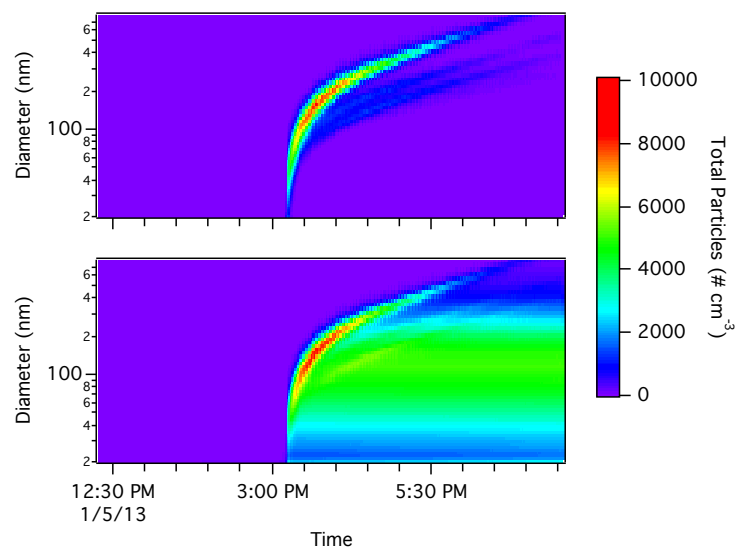


Figure S.6. Uncorrected (top) and wall loss corrected (bottom) aerosol growth events from a representative experiment (α -pinene + O_3).

Characterization of SEMS precision

To assess the precision of the SEMS measurement and reproducibility of our experimental protocol, we conducted two replicate α -pinene + O_3 experiments. Since they are O_3 -only experiments, we do not have a way to constrain the uncertainty on ΔHC , so we assume that all uncertainty on the aerosol mass yield is due to the precision of the ΔM measurement. To calculate the relative error on this measurement, we interpolated the total mass time series from each of these two experiments onto a common ΔHC trace. From these two interpolated ΔM traces, we could calculate the average ΔM and standard deviation, which provided the relative error trace shown in Figure S.7. The relative error was not constant with ΔHC , so we conservatively chose the highest stable value (15 %) to use as the error on ΔM for all experiments.

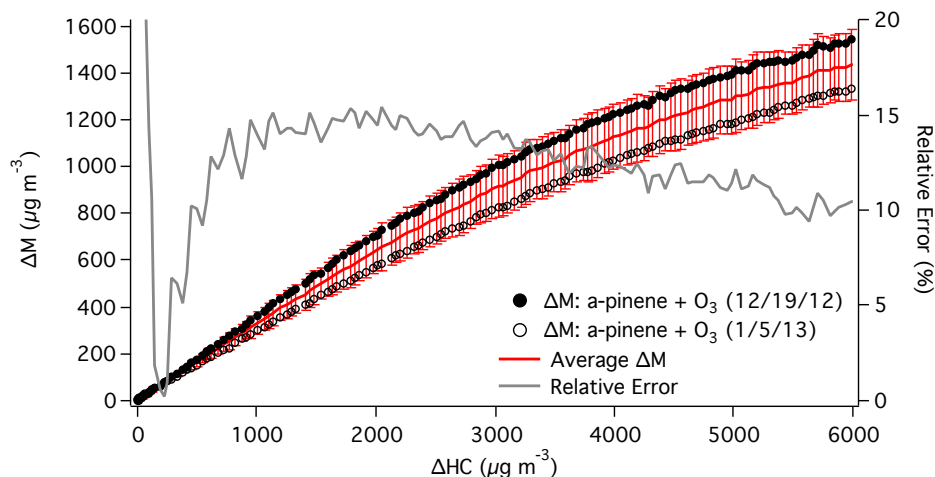


Figure S.7. The average and standard deviation of ΔM at a given amount of reacted hydrocarbon were calculated (red trace) from two replicate measurements of α -pinene + O_3 made in the REC (black circles). The standard deviation was used to calculate the relative error associated with ΔM measurements (grey trace). Relative error on ΔM was not constant over the course of each full experiment, so we conservatively take the highest stable value – 15 % – as the relative error on ΔM for all experiments.

Individual Oxidant Contributions: Δ -carene and limonene

Figure S.8 is an extension of Figure 5 in the main text showing qualitatively similar behavior from both Δ -carene and limonene to β -pinene insofar as all three monoterpenes produce some aerosol mass during the period of the experiment kinetically dominated by NO_3 oxidation. Additionally, the minimum in peroxyxynitrate formation correlates well with the initiation of aerosol formation in all but the Δ -carene with medium NO_2 experiment.

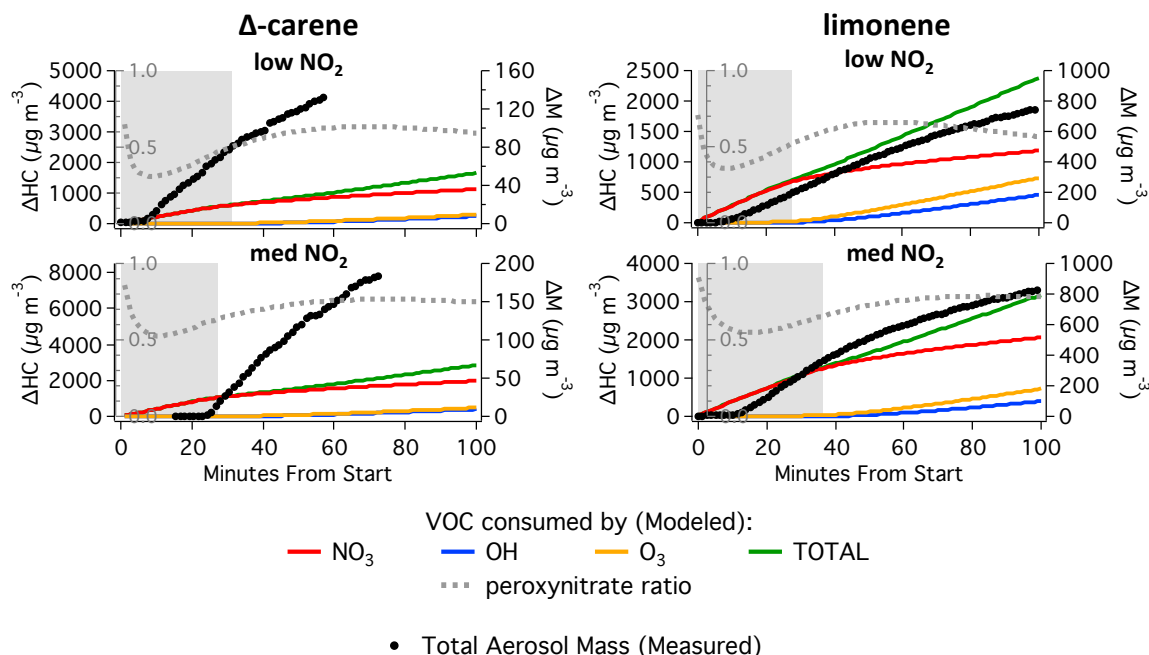


Figure S.8. Time series of wall loss corrected aerosol mass (right axis) and VOC consumed by each oxidant (left axis) for Δ^3 -carene and limonene at low and medium NO_2 concentrations, highlighting how much aerosol is produced at times dominated by NO_3 -oxidation (shaded regions). ΔHC values shown are the lower limits calculated using the lowest RO_2+RO_2 rate constant ($10^{-15} \text{ cm}^3 \text{ molec}^{-1} \text{ s}^{-1}$), which gives the low limit on how much NO_3 reacts with VOC directly. Dashed grey traces (inner left grey axis) represent the ratio of RO_2+NO_2 products that are present in the chamber (instantaneous concentration) relative to the sum of the instantaneous concentrations of RO_2+RO_2 , RO_2+NO_3 , and RO_2+NO_2 products. This ratio is a representation of the time dependence of peroxynitrate formation in the chamber.

Identification of products from HPLC-ESI-MS

Chromatographic separation coupled to high resolution mass spectrometry allows for relatively straightforward identification of products. A list of compounds was generated for each experiment from both positive and negative ion modes, using Agilent MassHunter software and employing a minimum relative intensity threshold of 1.5% of the highest intensity peak. Compound lists were then manually adjusted to ensure accurate ion adduct assignments, removal of redundant adducts at identical retention times, and formula assignments with consistent relative mass error. Although the product threshold was governed by relative intensity instead of an absolute cutoff, each of the software-identified products was manually searched for, at the same retention time, in the other experiments studying the same monoterpene. If any of those products were not identified by the software, but present at >3000 counts, they were added back to the product list for that experiment. This was done to minimize reporting NO_3 products that “are not formed” by O_3 oxidation, and vice versa, if they are formed but were missed by the software. Table S.2 shows the complete list of products included in Table 6 and

Figure 7. Table S.3 lists the most intense peaks and includes proposed structures according to specific products other studies have identified in similar systems as well as speculative structures simply showing that some of the high molecular weight products observed could be reasonably formed via oligomerization reactions of known monomers from these systems.

Table S.2. SOA compound formulae identified by HPLC-ESI-MS. Tables organized into O₃ and NO₃ regimes for each monoterpene, where any compound present in both oxidant regimes is only listed in the O₃ regime. Unless otherwise stated (see notes), compounds were observed only in the positive ion mode. Masses and formulae refer to the precursor (non-adduct) compound, which is reported as the nominal mass for any adducts misassigned by the software.

α-pinene + O₃				
Mass	Formula	Relative Mass Difference (MFG)	RT	Notes
184.1115	C10 H16 O3	-8.32	7.1	b
106.079	C8 H10	-6.91	7.184	
168.117	C10 H16 O2	-11.65	7.212	
182.1328	C11 H18 O2	-11.42	7.213	
168	C10 H16 O2	-13.15	8.685	
168	C10 H16 O2	-7.64	9.109	
152.1214	C10 H16 O	-8.47	9.377	
376.193	C21 H28 O6	-11.76	10.238	
243.1852	C13 H25 N O3	-7.36	11.029	b
421	C21 H27 N O8	-10.33	11.67	b
289.2647	C16 H35 N O3	-10.5	11.877	
216.1756	C12 H24 O3	-14.1	11.971	
128.121	C8 H16 O	-6.74	11.971	
287.2863	C17 H37 N O2	-13.31	11.982	
229.2437	C14 H31 N O	-13.81	12.022	
216.1755	C12 H24 O3	-13.78	12.027	
287.285	C17 H37 N O2	-9.01	12.242	
240.0714	C10 H12 N2 O5		12.694	c
276.1769	C17 H24 O3	-15.91	12.697	
220.1128	C13 H16 O3	-13.08	12.697	
466	C33 H22 O3	5.57	12.716	c
342.152	C20 H22 O5	-15.27	13.145	a
148.0178	C8 H4 O3	-11.81	13.293	d
278.1553	C16 H22 O4	-12.67	13.294	d
204.0815	C12 H12 O3	-13.98	13.294	d
278.1554	C16 H22 O4	-12.79	13.454	d
148.0179	C8 H4 O3	-12.3	13.455	d
228.2052	C14 H28 O2	16.29	13.528	c

- a) Peak only appears in O₃ experiment.
- b) Peak present in both positive and negative ion mode.
- c) Peak present in negative ion mode only.
- d) Known phthalate impurity.

α-pinene + NO₃ (excluding products listed in α -pinene + O ₃)				
Mass	Formula	Relative Mass Difference (MFG)	RT	Notes
186.0863	C ₉ H ₁₄ O ₄	15.8	5.802	c
138.106	C ₉ H ₁₄ O	-10.84	7.1	
114.0692	C ₆ H ₁₀ O ₂	-9.8	7.1	
213	C ₁₀ H ₁₅ N O ₄	-11.54	9.763	
201	C ₉ H ₁₅ N O ₄	-14.11	9.951	
152.1207	C ₁₀ H ₁₆ O	-3.79	11.236	
215	C ₁₀ H ₁₇ N O ₄	-10.25	11.236	
231	C ₁₀ H ₁₇ N O ₅	-12.33	11.315	
366	C ₂₀ H ₃₀ O ₆	-12.89	11.684	
310	C ₁₈ H ₃₀ O ₄	-11.55	11.867	
260	C ₁₀ H ₁₆ N ₂ O ₆	-10.05	12.135	
383.1987	C ₁₉ H ₂₉ N O ₇	-11.09	13.433	b
256.2363	C ₁₆ H ₃₂ O ₂	15.18	17.179	c,
215.0551	C ₁₂ H ₉ N O ₃	14.75	11.425	c
229.2426	C ₁₄ H ₃₁ N O	-9.08	11.857	
276.176	C ₁₇ H ₂₄ O ₃	-12.47	12.434	

- a) Peak only appears in O₃ experiment.
b) Peak present in both positive and negative ion mode.
c) Peak present in negative ion mode only.
d) Known phthalate impurity.

β-pinene + O₃				
Mass	Formula	Relative Mass Difference (MFG)	RT	Notes
186.091	C ₉ H ₁₄ O ₄	-9.51	5.902	
154.1001	C ₉ H ₁₄ O ₂	-4.94	5.923	
169.1112	C ₉ H ₁₂ O ₂	-5.26	6.125	
94.0789	C ₇ H ₁₀	-7.3	6.952	
108.0942	C ₈ H ₁₂	-2.54	6.953	
154.0998	C ₉ H ₁₄ O ₂	-2.87	6.954	
184.111	C ₁₀ H ₁₆ O ₃	-5.5	7.1	b
182.1315	C ₁₁ H ₁₈ O ₂	-4.44	7.21	
168.1159	C ₁₀ H ₁₆ O ₂	-5.42	7.211	
154.0999	C ₉ H ₁₄ O ₂	-3.27	7.579	
170	C ₁₀ H ₁₈ O ₂	-5.75	8.861	
138.1048	C ₉ H ₁₄ O	-2.59	9.058	
82.0427	C ₅ H ₆ O	-10.45	9.06	
358	C ₁₇ H ₂₆ O ₈	-8.98	9.231	a, b
138.1053	C ₉ H ₁₄ O	-5.79	9.286	
170	C ₁₀ H ₁₈ O ₂	-6.1	9.348	
376.1919	C ₂₁ H ₂₈ O ₆	-8.85	10.24	

370.2015	C19 H30 O7	-6.22	10.782	a, b
243.1849	C13 H25 N O3	-6.05	11.03	b
421	C21 H27 N O8	-8.43	11.673	b
287.2845	C17 H37 N O2	-7.21	11.985	
287.284	C17 H37 N O2	-5.3	12.245	
240.0706		14.02	12.695	a, c
278.1537	C16 H22 O4	-6.77	13.293	d
148.0165	C8 H4 O3	-3.24	13.293	d
278.1536	C16 H22 O4	-6.56	13.452	d
148.0164	C8 H4 O3	-2.41	13.452	d
204.0803	C12 H12 O3	-8.04	13.453	d
256.2354	C16 H32 O2	18.66	17.254	c

- a) Peak only appears in O₃ experiment.
b) Peak present in both positive and negative ion mode.
c) Peak present in negative ion mode only.
d) Known phthalate impurity.

β-pinene + NO₃ (excluding products listed in β-pinene + O ₃)				
Mass	Formula	Relative Mass Difference (MFG)	RT	Notes
170	C10 H18 O2	-2.67	7.173	
227.0811	C10 H13 N O5	-7.5	8.255	
245.0857	C10 H15 N O6	17.12	8.901	c
229	C10 H15 N O5	-4.38	9.245	
186	C10 H18 O3	-1.84	9.614	
264.133	C10 H20 N2 O6	-3.33	9.644	
230.1281	C10 H18 N2 O4	-6.15	9.767	
277.1107	C11 H19 N O7	19.83	9.789	c
184.1059	C10 H16 O3		10.358	c
227.1904	C13 H25 N O2	-8.17	11.107	
229.0909	C10 H15 N O5	17.94	11.226	c
230.1278	C10 H18 N2 O4	-4.77	11.233	
215	C10 H17 N O4	-2.94	11.241	
197.1066	C10 H15 N O3	-7.08	11.382	
215	C10 H17 N O4	-2.5	11.382	
134.1094	C10 H14	0.92	11.382	
156.1117			11.386	c
96.0581	C6 H8 O	-5.97	11.386	
152.1197	C10 H16 O	2.44	11.386	
217.1685	C11 H23 N O3	-3.26	11.415	
215.054	C12 H9 N O3	19.61	11.434	c
215	C10 H17 N O4	-3.42	11.537	
277.1109	C11 H19 N O7	18.8	11.734	c
231	C10 H17 N O5	-2.01	11.742	

260.1382	C11 H20 N2 O5	-3.77	11.944	
260	C10 H16 N2 O6	-3.69	12.139	
260	C10 H16 N2 O6	-3.16	12.722	
397.2037	C20 H31 N O7	15.95	13.802	c
383.1882	C19 H29 N O7	16.06	13.845	c
430.2329	C20 H34 N2 O8	-3.11	14.298	
413.1976	C20 H31 N O8	17.88	14.316	c
413	C21 H35 N O7	-3.6	14.858	
385	C19 H31 N O7	-4.71	15.6	
429	C21 H35 N O8	-3.15	15.608	
431.209	C20 H33 N O9	15.11	15.629	c
415	C20 H33 N O8	-5.37	15.895	
442	C20 H30 N2 O9	-4.83	15.977	
428.2174	C20 H32 N2 O8	-3.65	16.684	b
444	C20 H32 N2 O9	-5.54	16.807	
460	C20 H32 N2 O10	-2.88	17.298	

- a) Peak only appears in O₃ experiment.
b) Peak present in both positive and negative ion mode.
c) Peak present in negative ion mode only.
d) Known phthalate impurity.

Δ-carene + O₃				
Mass	Formula	Relative Mass Difference (MFG)	RT	Notes
154.098	C9 H14 O2	8.63	6.676	a
186.0886	C9 H14 O4	3.12	7.494	a, c
184.1086	C10 H16 O3	7.32	7.706	b
114.0675	C6 H10 O2	5.22	7.73	
184.1094	C10 H16 O3	3.15	8.155	c
222.1209	C11 H20 O3	10.28	8.211	
184.1086	C10 H16 O3	7.33	8.28	
138.1032	C9 H14 O	8.99	8.311	
200	C11 H20 O3	7.55	8.434	
92.0631	C7 H8	-4.95	8.44	
122.1089	C9 H14	5.05	8.442	
106.0777	C8 H10	5.1	8.445	
168.1137	C10 H16 O2	7.62	8.45	
201.1353	C10 H16 O3	5.94	9.029	
138.1032	C9 H14 O	9.16	9.049	
168	C10 H16 O2	9.3	9.263	
168	C10 H16 O2	7.51	9.418	
168.1139	C10 H16 O2	6.93	9.523	
170	C10 H18 O2	6.74	10.032	
222.0882	C12 H14 O4	4.33	11.021	

243.1813	C13 H25 N O3	8.63	11.482	b
294.1457	C16 H22 O5	3.55	11.833	a
287.2808	C17 H37 N O2	5.53	12.356	
287.2807	C17 H37 N O2	6.09	12.609	
220.1082	C13 H16 O3	7.97	13.055	
160.0875	C9 H14 O		13.055	
276.1708	C17 H24 O3	6.4	13.056	
148.0147	C8 H4 O3	9.37	13.681	d
278.1501	C16 H22 O4	6.25	13.682	d
222.0881	C12 H12 O3		13.683	a, d
148.0141	C8 H4 O3	12.97	13.856	d
278.1504	C16 H22 O4	5.1	13.865	d

- a) Peak only appears in O₃ experiment.
b) Peak present in both positive and negative ion mode.
c) Peak present in negative ion mode only.
d) Known phthalate impurity.

Δ-carene + NO₃ (excluding products listed in Δ-carene + O₃)				
Mass	Formula	Relative Mass Difference (MFG)	RT	Notes
186.0878	C9 H14 O4	7.6	6.51	c
172.1084	C9 H16 O3	9.06	6.946	
152.1186	C10 H16 O	9.66	7.13	
199.1193	C10 H17 N O3	7.64	7.33	
110.0725	C7 H10 O	5.7	7.498	
168.1137	C10 H16 O2	8.21	7.499	
140.0825	C8 H12 O2	9.09	7.514	
211.155	C12 H21 N O2	10.39	7.541	
70.0419	C4 H6 O	-0.86	7.731	
138.1034	C9 H14 O	7.44	7.731	
211.1548	C12 H21 N O2	11.61	8.475	
227.0772	C10 H13 N O5	9.7	8.873	
108.0566	C7 H8 O	8.81	9.298	
200	C10 H16 O4	8.31	9.406	
199	C9 H13 N O4	9.7	10.178	
380.1585	C18 H24 N2 O7	-0.52	10.626	
229.1663	C12 H23 N O3	6.37	10.737	
168	C10 H16 O2	11.79	10.886	
168	C10 H16 O2	11.36	11.097	
358.176	C21 H26 O5	4.25	11.797	
215	C10 H17 N O4	10.75	11.853	
134.1072	C10 H14	17.16	11.855	
200	C11 H20 O3	14.23	11.863	

472.1599	C21 H28 O12	3.94	11.874	
215	C10 H17 N O4	9.89	11.966	
168.1134	C10 H16 O2	9.98	12.058	
152.1187	C10 H16 O	9.42	12.059	
215	C10 H17 N O4	9.99	12.061	
182.1285	C11 H20 O3	11.75	12.079	
243	C11 H17 N O5	11.82	12.363	
400.187	C23 H28 O6	3.9	12.48	
564.1592	C25 H28 N2 O13	-0.17	12.722	
190.0977	C10 H16 O2		12.8	
340.1651	C21 H24 O4	6.91	12.803	
478.2132	C20 H34 N2 O11	6.42	13.748	
312.1332	C19 H20 O4	9.43	13.791	
418.2283	C19 H34 N2 O8	7.68	13.837	
204.0769	C12 H12 O3	8.34	13.893	d
476	C20 H32 N2 O11	4.91	14.72	
413	C20 H31 N O8	5.94	14.772	
413	C20 H31 N O8	5.48	14.932	
476	C20 H32 N2 O11	4.11	15.309	
476	C20 H32 N2 O11	4.2	15.501	

- a) Peak only appears in O₃ experiment.
b) Peak present in both positive and negative ion mode.
c) Peak present in negative ion mode only.
d) Known phthalate impurity.

limonene + O ₃				
Mass	Formula	Relative Mass Difference (MFG)	RT	Notes
154.0972	C9 H14 O2	14.38	5.616	
186.0868	C9 H14 O4	13.14	7.438	
80.0619	C6 H8	8.6	7.438	
126.0669	C7 H10 O2	9.43	7.441	
186.0871	C9 H14 O4	11.07	7.701	b
184.1072	C10 H16 O3	14.71	7.754	
184.1075	C10 H16 O3	13.27	8.373	b
200	C11 H20 O3	12.66	8.667	
92.0625	C7 H8	1.56	8.674	
132.0921	C10 H12	13.52	8.682	
122.1083	C9 H14	10.11	8.684	
168.1129	C10 H16 O2	12.91	8.685	
106.077	C8 H10	11.72	8.685	
188	C9 H16 O4	12.51	9.177	
222.0864	C12 H14 O4	12.68	11.064	
157.1446	C9 H19 N O	13.25	11.205	

243.1803	C13 H25 N O3	12.85	11.518	b
287.2792	C17 H37 N O2	11.17	12.392	
128.1183	C8 H16 O	14.21	12.399	
216	C12 H24 O3	11.07	12.406	
287.2789	C17 H37 N O2	12.16	12.649	
314	C18 H34 O4	14.78	13.084	
276.1702	C17 H24 O3	8.54	13.091	
220.1072	C13 H16 O3	12.36	13.099	
330.1774	C18 H28 O4	9.89	13.105	
300.1657	C14 H24 N2 O5	9.51	13.226	
358	C20 H38 O5	11.94	13.312	
278.1487	C16 H22 O4	11.26	13.732	d
148.0138	C8 H4 O3	15.22	13.732	d
222.087	C12 H14 O4	9.87	13.732	a
312.1314	C19 H20 O4	15.22	13.819	
278.1491	C16 H22 O4	9.8	13.918	d
286.2102	C16 H30 O4	14.65	14.828	
402.2203	C20 H34 O8	12.51	15.376	

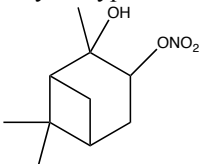
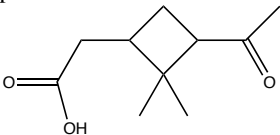
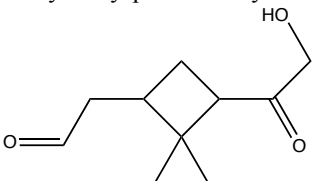
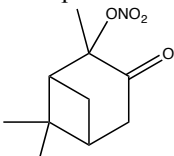
- a) Peak only appears in O₃ experiment.
b) Peak present in both positive and negative ion mode.
c) Peak present in negative ion mode only.
d) Known phthalate impurity.

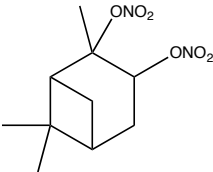
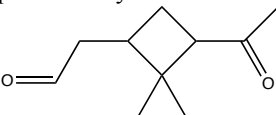
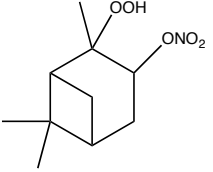
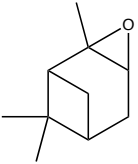
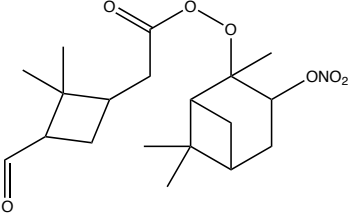
limonene + NO₃ (excluding products listed in limonene + O ₃)				
Mass	Formula	Relative Mass Difference (MFG)	RT	Notes
245.0868	C10 H15 N O6	12.7	5.916	
154.097	C9 H14 O2	15.36	6.171	
217.092	C9 H15 N O5	13.76	6.584	b
279	C10 H17 N O8	13.3	6.658	b
215	C9 H13 N O5	13.8	7.522	
217.0921	C9 H15 N O5	12.87	8.491	
227.076	C10 H13 N O5	15.01	8.892	
168.1124	C10 H16 O2	15.8	9.381	
245	C10 H15 N1 O6	12.95	9.934	
278.0727	C9 H14 N2 O8	8.17	10.094	c
294.1041	C10 H18 N2 O8	7.42	10.148	c
310.0985	C10 H18 N2 O9	8.93	10.292	c
338.0937	C11 H18 N2 O10	7.19	10.331	c
524.182	C20 H32 N2 O14	6.4	10.568	c
380.1558	C18 H24 N2 O7	6.74	10.664	
176.045	C10 H8 O3	13.57	11.066	
292.1277	C16 H20 O5	11.45	11.694	

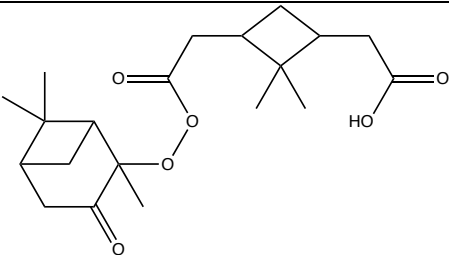
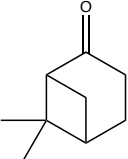
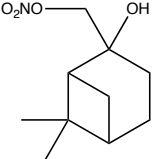
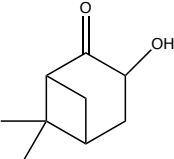
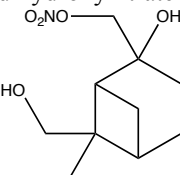
358.1737	C21 H26 O5	11.98	11.834	
472.1564	C27 H24 N2 O6	14.98	11.913	
280.0698	C17 H12 O4	13.32	12.035	
492	C20 H32 N2 O12	8.62	12.127	
555	C20 H33 N3 O15	10.67	12.187	b
432	C18 H28 N2 O10	8.23	12.245	
290.1823	C16 H28 O3	12.04	12.387	
236.1743	C15 H24 O2	14.2	12.389	
492	C20 H32 N2 O12	8.22	12.428	
432	C18 H28 N2 O10	9.88	12.495	
492.1912	C20 H32 N2 O12	8.77	12.528	
218.1639	C15 H24 O2	14.48	12.536	
190.0965	C12 H14 O2	15.27	12.839	
432	C18 H28 N2 O10	9.19	12.84	
340.1631	C21 H24 O4	13.12	12.84	
446	C19 H30 N2 O10	9.82	12.917	
432	C18 H28 N2 O10	10.16	13.009	
509	C19 H31 N3 O13	7.32	13.131	
446	C19 H30 N2 O10	9.82	13.192	
509	C19 H31 N3 O13	7.66	13.34	
446	C19 H30 N2 O10	9.84	13.342	
523	C20 H33 N3 O13	9.27	13.366	
258.1795	C14 H26 O4	13.94	13.515	
476	C20 H32 N2 O11	8.29	13.518	
523	C20 H33 N3 O13	8.02	13.564	
482.1834	C20 H32 N2 O10	8.71	13.712	
446	C19 H30 N2 O10	8.84	13.788	
446	C19 H30 N2 O10	9.18	13.915	
204.076	C12 H12 O3	12.92	13.927	d
523	C20 H33 N3 O13	8.38	14.278	
460	C20 H32 N2 O10	9.33	14.304	
523	C20 H33 N3 O13	8.98	14.434	
358.2446	C18 H34 N2 O5	5.98	14.871	
304.2374	C20 H32 O2		14.871	

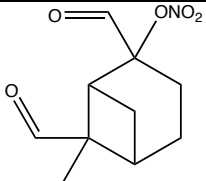
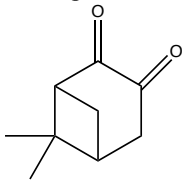
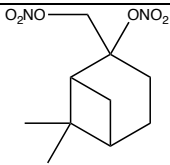
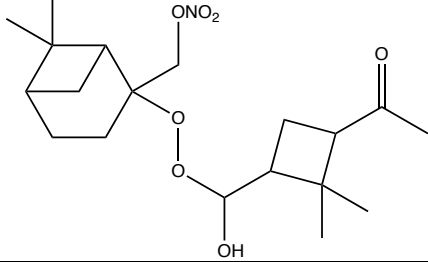
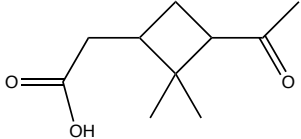
- a) Peak only appears in O₃ experiment.
- b) Peak present in both positive and negative ion mode.
- c) Peak present in negative ion mode only.
- d) Known phthalate impurity.

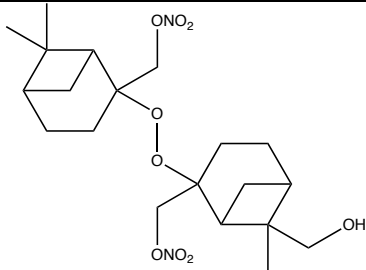
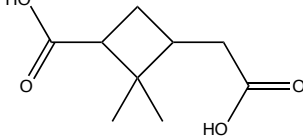
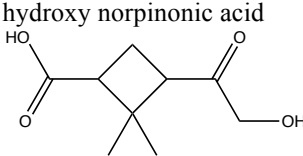
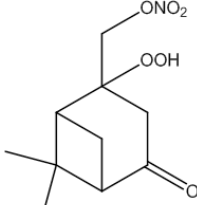
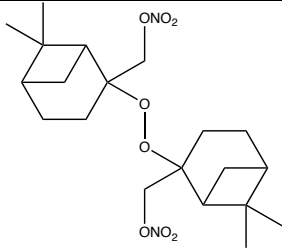
Table S.3. Masses and elemental composition for (a) all peaks with intensity greater than 10% of the strongest peak observed in any of the ESI-MS spectra for each BVOC, (b) additional molecular formulae that have been identified by other studies, and (c) selected high-mass peaks. Possible molecular structures, which may be isomers of the true structure, are listed for most molecular formulae. As in Table S.2, masses and formulae refer to the precursor (non-adduct) compound, which is reported as the nominal mass for any adducts misassigned by the software.

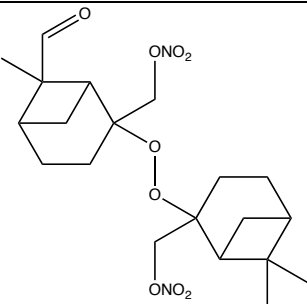
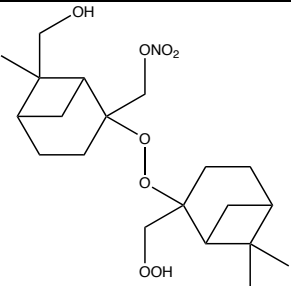
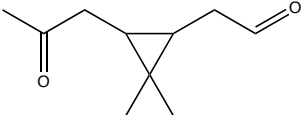
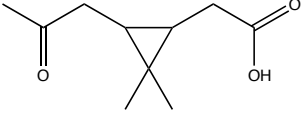
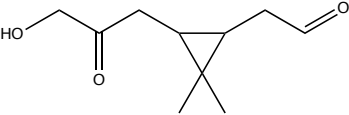
Measured m/z	Relative abundance	Oxidants observed with	Molecular formula	Possible structures	References (if previously observed)
α-pinene					
(a) 215	1	NO ₃	C ₁₀ H ₁₇ NO ₄	2-hydroxypinane-3-nitrate 	NO ₃ : Wangberg et al. (1997), Perraud et al. (2010), Ayres et al, in prep (2015)
184.1115	0.51	NO ₃	C ₁₀ H ₁₆ O ₃	pinonic acid  10-hydroxy-pinonaldehyde  & isomers	O ₃ : Yu et al. (1999), Glasius et al. (2000), Doezema et al. (2012) NO ₃ : Perraud et al. (2010)
213	0.15	NO ₃	C ₁₀ H ₁₅ N O ₄	3-oxopinane-2-nitrate 	NO ₃ : Wangberg 1997, Perraud 2010

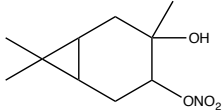
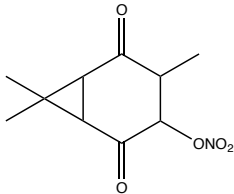
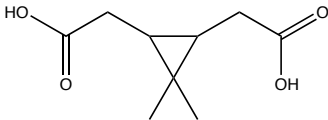
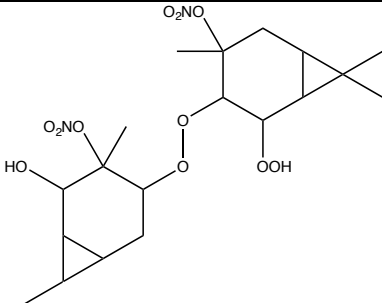
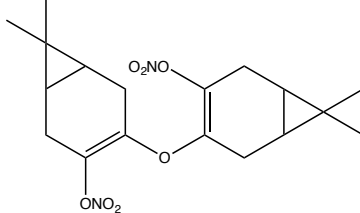
260	0.15	NO ₃	C10 H16 N2 O6	2,3-dinitrato-pinane 	
(b) 168.1166	0.08, 0.04	NO ₃ , O ₃	C10 H16 O2	pinonaldehyde 	O ₃ : Glasius 2000, Yu 1999, Doezema et al. (2012) NO ₃ : Wangberg et al. (1997), Hallquist et al. (1999), Perraud et al. (2010)
231	0.07	NO ₃	C10 H17 N O5	2-hydroperoxypinane-3-nitrate 	NO ₃ : Ayres et al, in prep (2015)
152.1214	0.05, 0.02	NO ₃ , O ₃	C10 H16 O	pinane epoxide 	NO ₃ : Wangberg et al. (1997)
(c) 383.1987	0.08	NO ₃	C19 H29 N O7		speculative, loosely following Heaton et al. (2007)

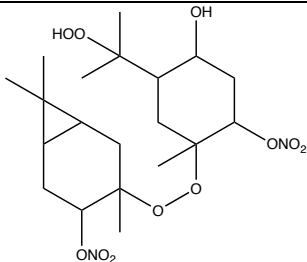
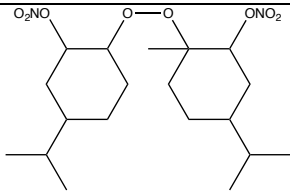
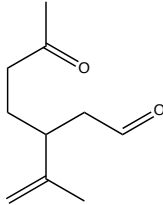
366	0.05	NO ₃	C ₂₀ H ₃₀ O ₆		speculative
β-pinene					
(a) 138.1048	0.47, 0.49	NO ₃ , O ₃	C ₉ H ₁₄ O	nopinone 	O ₃ : Glasius et al. (2000), Yu et al. (1999) NO ₃ : Hallquist et al. (1999)
215	0.43	NO ₃	C ₁₀ H ₁₇ N O ₄	hydroxynitrate 	NO ₃ : Fry et al. (2009), Ayres in prep (2015)
154.0999	0.29, 0.30	NO ₃ , O ₃	C ₉ H ₁₄ O ₂	hydroxypinaketone 	O ₃ : Glasius et al. (2000), Yu et al. (1999)
429	0.28	NO ₃	C ₂₁ H ₃₅ N O ₈		
231	0.27	NO ₃	C ₁₀ H ₁₇ N O ₅	dihydroxynitrate 	NO ₃ : Fry et al. (2009), Ayres in prep (2015)

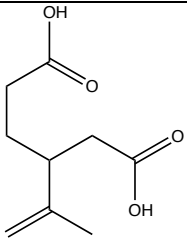
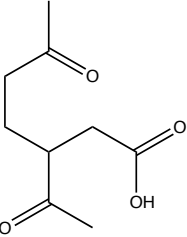
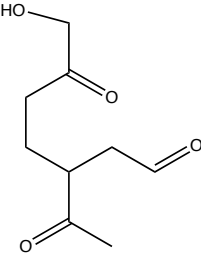
227.0803	0.23	NO ₃	C ₁₀ H ₁₃ N O ₅		speculative
152.0842	0.18	NO ₃	C ₉ H ₁₂ O ₂	3-oxo-pinaketone 	O ₃ : Yu et al. (1999)
230.1276	0.14	NO ₃	C ₁₀ H ₁₈ N ₂ O ₄		
260	0.13	NO ₃	C ₁₀ H ₁₆ N ₂ O ₆		
385	0.13	NO ₃	C ₁₉ H ₃₁ N O ₇		speculative, loosely following Heaton et al. (2007)
429	0.11	NO ₃	C ₂₁ H ₃₅ N O ₈		
184.1102	0.11. 0.03	NO ₃ , O ₃	C ₁₀ H ₁₆ O ₃	pinonic acid 	O ₃ : Glasius et al. (2000)

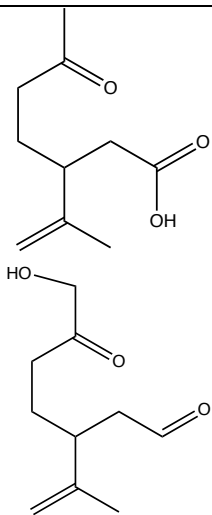
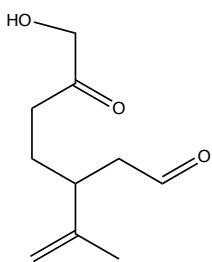
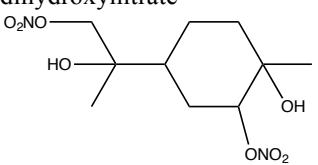
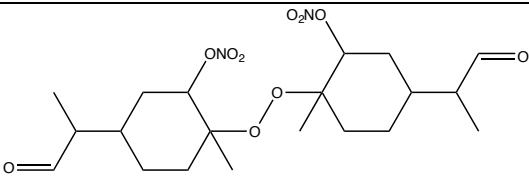
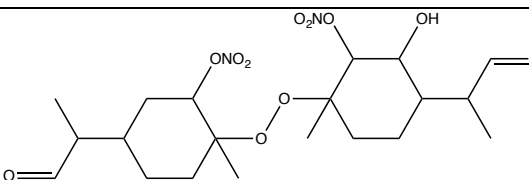
444	0.10	NO ₃	C ₂₀ H ₃₂ N ₂ O ₉		speculative
(b) 186.0905	0.03, 0.02	NO ₃ , O ₃	C ₉ H ₁₄ O ₄	<p>pinic acid</p>  <p>hydroxy norpinonic acid</p> 	O ₃ : Glasius et al. (2000), Yu et al. (1999)
245.0857	<i>Neg ion mode</i>	NO ₃	C ₁₀ H ₁₅ N O ₆		NO ₃ : Ng et al, ACPD (2015)
(c) 428.2174	0.05	NO ₃	C ₂₀ H ₃₂ N ₂ O ₈		speculative

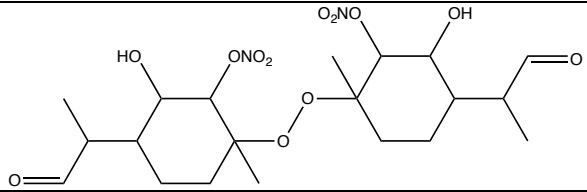
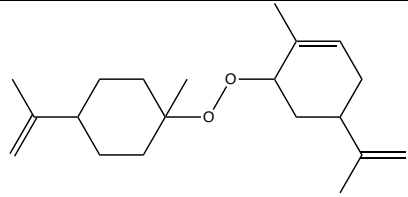
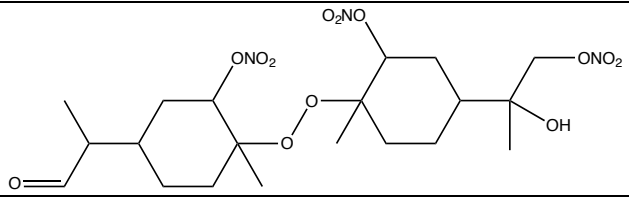
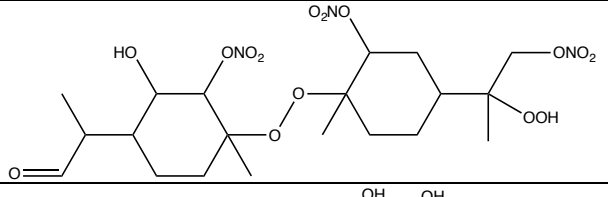
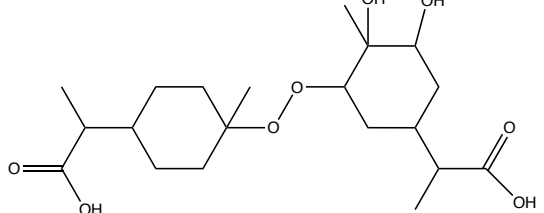
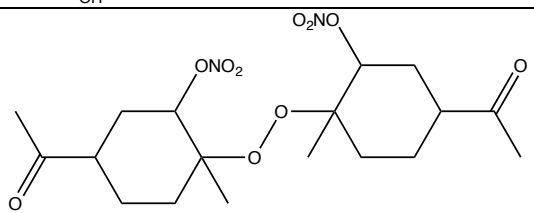
442	0.04	NO ₃	C20 H30 N2 O9		speculative
415	0.03	NO ₃	C20 H33 N O8		speculative
Δ-carene					
(a) 168.1137	0.17, 0.60	NO ₃ , O ₃	C10 H16 O2	caronaldehyde 	O ₃ : Glasius et al. (2000) NO ₃ : Hallquist et al. (1999)
340.1651	0.57	NO ₃	C21 H24 O4		
184.1076	0.33, 0.12	NO ₃ , O ₃	C10 H16 O3	3-caronic acid  10-hydroxy-3-caronaldehyde 	O ₃ : Glasius et al. (2000)
200	0.26	O ₃	C11 H20 O3		

215	0.25	NO ₃	C10 H17 N O4	hydroxynitrate 	NO ₃ : Colville and Griffin (2004), Ayres in prep (2015)
227.0772	0.13	NO ₃	C10 H13 N O5		very speculative !
276.1708	0.12	NO ₃	C17 H24 O3		
243.1813	0.11	NO ₃	C13 H25 N O3		
186.0886	<i>Neg ion mode</i>		C9 H14 O4	3-caric acid 	O ₃ : Glasius et al. (2000), Yu et al. (1999)
(c) 476	0.05	NO ₃	C20 H32 N2 O11		speculative
380.1585	0.04	NO ₃	C18 H24 N2 O7		Very speculative!
413	0.04	NO ₃	C20 H31 N O8		

478.2132	0.03	NO ₃	C ₂₀ H ₃₄ N ₂ O ₁₁		speculative – this formula is consistent with some ring-opening in the dimer
418.2283	0.03	NO ₃	C ₁₉ H ₃₄ N ₂ O ₈		speculative – also consistent with ring-opened products
limonene					
(a) 340.1631	0.37	NO ₃	C ₂₁ H ₂₄ O ₄	Extremely low H:C ratio, has to be very conjugated	
168.1125	0.30, 0.27	NO ₃ , O ₃	C ₁₀ H ₁₆ O ₂	limonaldehyde/endolim 	O ₃ : Glasius et al. (2000), Walser et al. (2008) NO ₃ : Spittler et al. (2006), Hallquist et al. (1999), Fry et al. (2011)

186.0868	0.12, 0.28	NO ₃ , O ₃	C ₉ H ₁₄ O ₄	<div> <div>limonic acid:</div>  </div> <div> <div>keto-limononic acid:</div>  </div> <div> <div>7-hydroxy-keto-limonaldehyde:</div>  </div>	O ₃ : Glasius et al. (2000), Walser et al. (2008)
182.128	0.15, 0.14	NO ₃ , O ₃	C ₁₁ H ₁₈ O ₂		
268	0.12	NO ₃	C ₁₆ H ₂₈ O ₃		

(b) 184.1075	0.02, 0.03	NO ₃ , O ₃	C ₁₀ H ₁₆ O ₃	<p>limononic acid:</p>  <p>7-hydroxy-limonaldehyde:</p> 	O ₃ : Glasius et al. (2000), Walser et al. (2008)
294.1041	0.01	NO ₃	C ₁₀ H ₁₈ N ₂ O ₈	<p>dihydroxynitrate</p> 	NO ₃ : Fry et al. (2011)
(c) 460	0.01	NO ₃	C ₂₀ H ₃₂ N ₂ O ₁₀		speculative, just intended to show possible dimer structures
476	0.01	NO ₃	C ₂₀ H ₃₂ N ₂ O ₁₁		“

492	0.01	NO ₃	C20 H32 N2 O12		“
304.2357	0.01	NO ₃	C20 H32 O2		“
523	0.01	NO ₃	C20 H33 N3 O13		“
555	0.01	NO ₃	C20 H33 N3 O15		“
402.2203	0.01	NO ₃	C20 H34 O8		“
432	0.04	NO ₃	C18 H28 N2 O10		“
* limonene spectra also contain several more analogous C18-C19 peaks.					

References

- Andres-Hernandez, M. D., Kartal, D., Crowley, J. N., Sinha, V., Regelin, E., Martinez Harder, M., Nenakhov, V., Williams, J., Harder, H., Bozem, H., Song, W., Thieser, J., Tang, M. J., Hosaynali Beigi, Z., Burrows, J. P.: Diel peroxy radicals in a semi-industrial coastal area: nighttime formation of free radicals, *Atmospheric Chemistry and Physics*, 13, 5731-5749, doi:10.5194/acp-13-5731-2013, 2013.
- Atkinson, R.: Atmospheric Reactions of Alkoxy and β -Hydroxyalkoxy Radicals, *International Journal of Chemical Kinetics*, 29, 99-111, doi: 10.1002/(SICI)10974601(1997)29:2<99::AID-KIN3>3.0.CO;2-F, 1997.
- Atkinson, R. and Arey, J.: Atmospheric Degradation of Volatile Organic Compounds, *Chemical Reviews*, 103, 4605-4638, doi:10.1021/cr0206420, <http://pubs.acs.org/doi/abs/10.1021/cr0206420>, 2003.
- Atkinson, R., Aschmann, S. M., Arey, J., and Shorees, B.: Formation of OH radicals in the gas phase reactions of O₃ with a series of terpenes, *Journal of Geophysical Research: Atmospheres*, 97, 6065-6073, doi:10.1029/92JD00062, <http://dx.doi.org/10.1029/92JD00062>, 1992.
- Atkinson, R.: Gas-Phase Tropospheric Chemistry of Volatile Organic Compounds: 1. Alkanes and Alkenes, *Journal of Physical and Chemical Reference Data*, 26, 215-290, doi:<http://dx.doi.org/10.1063/1.556012>, 1997.
- Atkinson, R., Baulch, D. L., Cox, R. A., Crowley, J. N., Hampson, R. F., Hynes, R. G., Jenkin, M. E., Rossi, M. J., and Troe, J.: Evaluated kinetic and photochemical data for atmospheric chemistry: Volume I - gas phase reactions of O_x, HO_x, NO_x and SO_x species, *Atmos. Chem. Phys.*, 4, 1461-1738, doi:10.5194/acp-4-1461-2004, 2004.
- Boyd, C. M., Sanchez, J., Xu, L., Eugene, A. J., Nah, T., Tuet, W. Y., Guzman, M. I., and Ng, N. L.: Secondary Organic Aerosol (SOA) formation from the β -pinene + NO₃ system: effect of humidity and peroxy radical fate, *Atmospheric Chemistry and Physics Discussion*, 15, 2679-2744, doi:10.5194/acpd-15-2679-2015, 2015.
- Colville, C. J. and Griffin, R. J.: The roles of individual oxidants in secondary organic aerosol formation from Δ^3 -carene: 1. gas-phase chemical mechanism, *Atmospheric Environment*, 38, 4001-4012, 2004.
- DeMore, W. G., Sander, S. P., Golden, D. M., Hampson, R. F., Kurylo, M. J., Howard, C. J., Ravishankara, A. R., Kolb, C. E., and Molina, M. J.: Chemical Kinetics and Photochemical Data for Use in Stratospheric Modeling, Evaluation Number 11, JPL Publication, 94-26, 1994.
- Doezema, L. A., Longin, T., Cody, W., Perraud, V., Dawson, M. L., Ezell, M. J., Greaves, J., Johnson, K. R., and Finlayson-Pitts, B. J.: Analysis of secondary organic aerosols in air using extractive electrospray ionization mass spectrometry (EESI-MS), *RSC Adv.*, 2, 2930-2938, doi:10.1039/C2RA00961B, 2012.

Ehn, M., Thornton, J. A., Kleist, E., Sipila, M., Junninen, H., Pullinen, I., Springer, M., Rubach, F., Tillmann, R., Lee, B., Lopez-Hilfiker, F., Andres, S., Acir, L.-H., Rissanen, M., Jokinen, T., Schobesberger, S., Kangasluoma, J., Kontkanen, J., Nieminen, T., Kurten, T., Nielsen, L. B., Jorgensen, S., Kjaergaard, H. G., Canagaratna, M., Maso, M. D., Berndt, T., Petaja, T., Wahner, A., Kerminen, V. M., Kulmala, M., Worsnop, D. R., Wildt, J., and Mentel, T. F.: A large source of low-volatility secondary organic aerosol, *Nature*, 506, 476-479, doi:10.1038/nature13032, 2014.

Fry, J. L., Kiendler-Scharr, A., Rollins, A. W., Woodridge, P. J., Brown, S. S., Fuchs, H., Dube, W., Mensah, A., dal Maso, M., Tillmann, R., Dorn, H. P., Brauers, T., and Cohen, R. C.: Organic nitrate and secondary organic aerosol yield from NO₃ oxidation of β -pinene evaluated using a gas-phase kinetics/aerosol partitioning model, *Atmospheric Chemistry and Physics*, 9, 1431-1449, doi:10.5194/acp-91431-2009, 2009.

Fry, J. L., Kiendler-Scharr, A., Rollins, A. W., Brauers, T., Brown, S. S., Dorn, H. P., Dube, W. P., Fuchs, H., Mensah, A., Rohrer, F., Tillmann, R., Wahner, A., Woodridge, P. J., and Cohen, R. C.: SOA from limonene: role of NO₃ in its generation and degradation, *Atmospheric Chemistry and Physics*, 11, 3879-3894, doi:10.5194/acp-11-3879-2011, 2011.

Fry, J. L., Draper, D. C., Barsanti, K. C., Smith, J. N., Ortega, J., Winkler, P. M., Lawler, M. J., Brown, S. S., Edwards, P. M., Cohen, R. C., and Lee, L.: Secondary Organic Aerosol Formation and Organic Nitrate Yield from NO₃ Oxidation of Biogenic Hydrocarbons, *Environmental Science & Technology*, 48, 11944-11953, doi:10.1021/es502204x, 2014.

Glasius, M., Lahaniati, M., Calogirou, A., Di Bella, D., Jensen, N. R., Hjorth, J., Kotzias, D., and Larsen, B. R.: Carboxylic Acids in Secondary Aerosols from Oxidation of Cyclic Monoterpenes by Ozone, *Environmental Science & Technology*, 34, 1001-1010, doi:10.1021/es990445r, 2000.

Hallquist, M., Wangberg, I., Ljungstrom, E., Barnes, I., and Becker, K. H.: Aerosol and Product Yields from NO₃ Radical-Initiated Oxidation of Selected Monoterpenes, *Environmental Science & Technology*, 33, 553-559, doi:10.1021/es980292s, 1999.

Haynes, W., Bruno, T. J., and Lide, D. R., eds.: CRC Handbook of Chemistry and Physics, 93rd Edition (Internet Version), CRC Press/Taylor and Francis, 2012.

Heaton, K. J., Dreyfus, M. A., Wang, S., and Johnston, M. V.: Oligomers in the Early Stage of Biogenic Secondary Organic Aerosol Formation and Growth, *Environmental Science & Technology*, 41, 6129-6136, doi:10.1021/es070314n, 2007.

Lightfoot, P. D., Cox, R. A., Crowley, J. N., Destriau, M., Hayman, G. D., Jenkin, M. E., Moortgat, G. K., Zabel, F.: Organic peroxy radicals: Kinetics, spectroscopy and tropospheric chemistry, *Atmospheric Environment Part A-General Topics*, 26, 1805-1961, doi:10.1016/0960-1686(92)90423-I, 1992.

McMurry, P. H. and Grosjean, D.: Gas and aerosol wall losses in Teflon film smog chambers, *Environmental Science and Technology*, 19, 1176-1182, doi:10.1021/es00142a006, 1985.

Orlando, J. J. and Tyndall, G. S.: Laboratory studies of organic peroxy radical chemistry: an overview with emphasis on recent issues of atmospheric significance, *Chem. Soc. Rev.*, 41, 6294-6317, doi:10.1039/c2cs35166h, 2012.

Perraud, V., Bruns, E. A., Ezell, M. J., Johnson, S. N., Greaves, J., and Finlayson-Pitts, B. J.: Identification of Organic Nitrates in the NO₃ Radical Initiated Oxidation of α -Pinene by Atmospheric Pressure Chemical Ionization Mass Spectrometry, *Environmental Science & Technology*, 44, 5887-5893, doi:10.1021/es1005658, 2010.

Sander, S., Abbatt, J., Barker, J. R., Burkholder, J. B., Friedl, R. R., Golden, D. M., Huie, R. E., Kolb, C. E., Kurylo, M. J., Moortgat, G. K., Orkin, V. L., and Wine, P. H.: Chemical Kinetics and Photochemical Data for Use in Atmospheric Studies, Evaluation Number 17, JPL Publication, 10, 2011.

Spittler, M., Barnes, L., Bejan, I., Brockmann, K., Benter, T., and Wirtz, K.: Reactions of NO₃ radicals with limonene and α -pinene: Product and SOA formation, *Atmospheric Environment*, 40, Supplement 1, 116-127, doi:10.1016/j.atmosenv.2005.09.093, 2006.

Vaughan, S., Canosa-Mas, C. E., Pfrang, C., Shallcross, D. E., Watson, L., Wayne, R. P.: Kinetic studies of reactions of the nitrate radical (NO₃) with peroxy radicals (RO₂): an indirect source of OH at night?, *Phys. Chem. Chem. Phys.*, 8, 3749-3760, doi:10.1039/b605569a, 2006.

Walser, M. L., Desyaterik, Y., Laskin, J., Laskin, A., and Nizkorodov, S. A.: Highresolution mass spectrometric analysis of secondary organic aerosol produced by ozonation of limonene, *Phys. Chem. Chem. Phys.*, 10, 1009-1022, doi:10.1039/B712620D, 2008.

Wangberg, I., Barnes, I., and Becker, K. H.: Product and Mechanistic Study of the Reaction of NO₃ Radicals with α -pinene, *Environmental Science & Technology*, 31, 2130-2135, doi:10.1021/es960958n, 1997.

Wolfe, G. M., Cantrell, C., Kim, S., Mauldin III, R. L., Karl, T., Harley, P., Turnipseed, A., Zheng, W., Flocke, F., Apel, E. C., Hornbrook, R. S., Hall, S. R., Ullmann, K., Henry, S. B., DiGangi, J. P., Boyle, E. S., Kaser, L., Schnitzhofer, R., Hansel, A., Graus, M., Nakashima, Y., Kajii, Y., Guenther, A., Keutsch, F. N.: Missing peroxy radical sources within a summertime ponderosa pine forest, *Atmospheric Chemistry and Physics*, 14, 4715-4732, doi:10.5194/acp-14-4715-2014, 2014.

Yu, J., Cocker, D., Griffin, R., Flagan, R., and Seinfeld, J.: Gas-phase ozone oxidation of monoterpenes: Gaseous and particulate products, *Journal of Atmospheric Chemistry*, 34, 207-258, 1999.

Zhang, J., Huff Hartz, K. E., Pandis, S. N. and Donahue, N. M.: Secondary Organic Aerosol Formation from Limonene Ozonolysis: Homogeneous and Heterogeneous Influences as a

Function of NO_x, *Journal of Physical Chemistry A*, 110(38), 11053–11063, doi:10.1021/jp062836f, 2006.

Ziemann, P. J., and Atkinson, R.: Kinetics, products, and mechanisms of secondary organic aerosol formation, *Chem. Soc. Rev.*, 41, 6582-6605, doi:10.1039/c2cs35122f, 2012.